LAWRENCE
LIVERMORE
NATIONAL
LABORATORY

LLNL-PROC-436491

Effect of non-axisymmetric magnetic perturbations on divertor profiles in NSTX H-mode plasmas

J. W. Ahn, J. Canik, R. Maingi, T. Gray, A. McLean, A. L. Roquemore, V. A. Soukhanovskii

June 16, 2010

The 37th EPS Conference on Plasma Physics
Dublin, Ireland
June 21, 2010 through June 25, 2010

Disclaimer

Effect of non-axisymmetric magnetic perturbations on divertor profiles in NSTX H-mode plasmas

J-W. Ahn[1], J.M. Canik[1], R. Maingi[1], T.K. Gray[1], A.G. McLean[1], A.L. Roquemore[2], and V.A. Soukhanovskii[3]

[1]*Oak Ridge National Laboratory, Oak Ridge, TN 37831, USA*
[2]*Princeton Plasma Physics Laboratory, Princeton, NJ 08543, USA*
[3]*Lawrence Livermore National Laboratory, Livermore, CA 94551, USA*

1. Introduction

It has been recently found that small, non-axisymmetric magnetic field perturbations produced by internal or external coils break the toroidal symmetry of divertor profiles in tokamaks, generating striated heat and particle deposition pattern at the divertor surface, e.g. in DIII-D [1] and NSTX [2]. This is a direct consequence of the 'strike point (SP) splitting' caused by the 3-D magnetic field perturbations to the plasma edge [3]. As many tokamak plasma facing components (PFCs) are designed and built assuming toroidal symmetry to protect areas where high heat and particle fluxes are expected from the 2-D equilibrium, this non-axisymmetric, *i.e.* 3-D, divertor profiles can result in additional engineering constraints. These applied 3-D magnetic perturbations are found to suppress [4] or mitigate [5] ELMs in conventional tokamaks, while they trigger ELMs in spherical tokamaks [6, 9]. In the National Spherical Torus Experiment (NSTX), the 3-D field perturbation was applied to ELM-free H-mode plasmas achieved with lithium wall coatings of the plasma facing components [7], in order to trigger controlled ELMs with the goal of flushing impurities and reducing radiated power from the core plasma [8]. It is therefore important to investigate the effect of 3-D field on heat and particle flux profiles during and between ELMs.

2. Experimental set-up and measurement technique

The 3-D perturbation fields on NSTX were generated with a set of six midplane coils that are typically used for error field correction. The coils were configured to apply an n=3 field in the ELM-destabilization experiments, with a generated magnetic perturbation at the separatrix, $\delta B/B$=0.6-0.7% for the peak δB at the coil center and on the order of 0.1% for the integrated δB over the coil surface. Heat flux measurements at the lower divertor target are made with a high speed (1.6-6.3kHz) infrared (IR) camera [9], installed at toroidal angle φ=135º (counter-clockwise from the reference, 225º if clockwise), with ~50º of field-of-view (FOV) at r=60cm giving the spatial resolution of 5-7mm. A 2-D heat conduction code,

THEODOR [10], is used to calculate the divertor heat flux profile from the measured surface temperature. However, the magnitude of the heat flux in this paper is uncertain because lithium coating changes the surface emissivity in an uncalibrated manner; relative profiles comparisons are valid, however. D_α emission at the lower divertor target is recorded by a 1-D CCD camera installed at φ=255º (counter-clockwise from the reference, 105º if clockwise). It is operated at a 2kHz rate and with sub-mm spatial resolution [11]. Note that we are using the D_α emission as a proxy for the particle flux in attached plasmas.

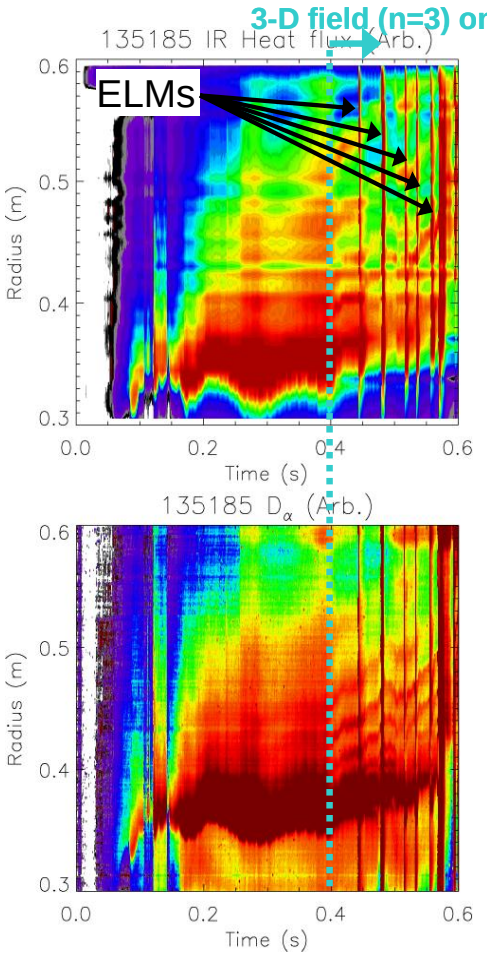

Figure 1. Contour plot of measured heat flux (upper) and D_α (lower) profiles with n=3 perturbation field applied from t=400ms.

3. Data analysis and interpretation

3.1 Strike point splitting with 3-D field application

The temporal and spatial evolution of the measured heat flux and D_α profiles for an applied n=3 perturbation in a lithium enhanced ELM-free H-mode discharge are shown in figure 1 as a contour plot. The striations in both profiles are formed shortly after the perturbation field initiation at 400ms. This striation represents the split strike points due to the applied 3-D fields; vacuum field line tracing reproduces the experimental observation quite well [2]. The inclusion of the plasma response inside the unperturbed separatrix by the Ideal Perturbed Equilibrium Code (IPEC) calculation [12] did not affect the structure of split strike points significantly, *i.e.*, the number and radial location of the generated lobes are unchanged relative to the vacuum field calculation. The toroidal displacement of the IR and D_α cameras by 120º is expected to produce n=3 periodicity in the divertor fluxes if the generated lobe structure is consistent with the imposed n=3 field structure. Indeed, the temporal and spatial evolution of striations is very similar for both heat flux and D_α profiles (see figure 1).

3.2 Intrinsic strike point splitting in relation with intrinsic error fields

Figure 1 also shows that the divertor flux profiles show a moderate level of strike point splitting even before the application of external magnetic perturbation. The profiles

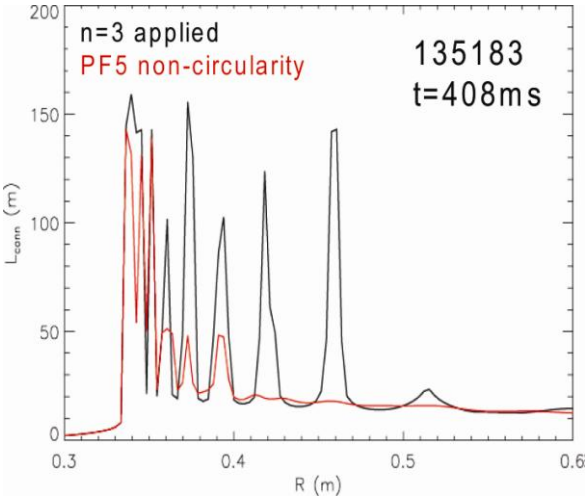

Figure 2. Comparison of computed connection length profile by the vacuum field line tracing between n=3 field applied case (black) and the PF5 intrinsic error field case (red)

show nearly monotonic decay, *i.e.*, no strike point splitting, until t~190ms and then begin to develop local peaks and valleys in the radial locations other than that of the original strike point at r~35cm. The degree of splitting varies in time, and both the heat flux and D_α profiles show similar evolution. As a possible source of the internal 3-D magnetic perturbation, the intrinsic error field from the non-circularity of PF5 coil was considered and included in the vacuum field line tracing. It was recently shown [13] that PF5 coil in NSTX produces error fields with n=3 component as a dominant component. The inclusion of PF5 non-circularity in the vacuum field line tracing is therefore expected to produce a dominant n=3 field structure although the model contains all non-circular components. Figure 2 shows a comparison of computed connection length profiles between the n=3 application and the PF5 intrinsic error field cases; the radial locations of the local peaks are in good agreement. This indicates that intrinsic error fields may be one of the sources of the intrinsic SP splitting. However, for many other discharges, the intrinsic SP splitting is not observed during the whole plasma duration time. It is unclear at present whether this is because the PF5 coil current in these discharges was too low (I_{PF5}=5.6kA) to produce SP splitting, compared to the other case (I_{PF5}=7.5kA), or the 2-D equilibrium fields superposed by the 3-D perturbation fields reacted toward the direction of canceling 3-D field effect.

3.3 Heat flux deposition during ELMs triggered by application of 3-D fields

Externally imposed 3-D fields trigger ELMs and strong heat and particle expulsion. Heat and particle release by the triggered ELMs onto the divertor surface is indicated by several vertical lines in figure 1. The frame speed of the IR camera was sufficiently high (~3.8kHz) to resolve heat flux profiles during the ELM. Figure 3 shows the calculated heat flux profiles at the ELM peak and immediately (0.6ms) before the ELM occurrence. One can notice that the SP splitting is persistent even during the ELM (t=444.6ms) as the profile exhibits local peaks and valleys. Also, the radial location of the split strike points before and during the ELM agrees with each other very well. This indicates that the heat flux profile from ELMs triggered by n=3 fields follows the imposed field structure, *i.e.*, 3-D field triggered ELMs appear to be phase locked to the externally applied perturbation. This has the important

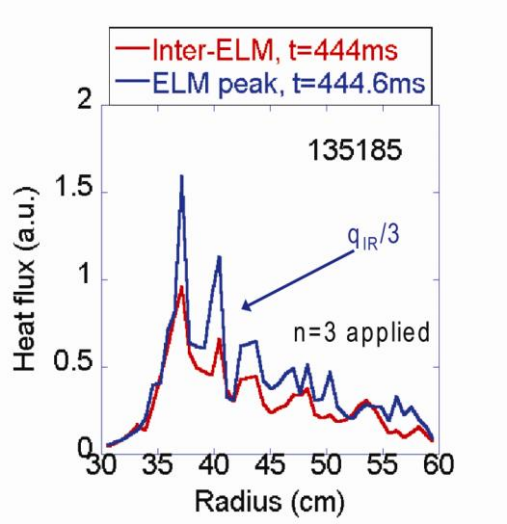

Figure 3. Heat flux profiles measured at the ELM peak (blue), divided by 3, and during the inter-ELM period, 0.6ms before the peak (red)

implication that the characteristics of the triggered ELMs might be determined by the imposed 3-D field structure.

In this paper, we showed that the vacuum field line tracing is good enough to predict the divertor profile modification in terms of the location and spacing of the striations caused by the applied 3-D fields. Our data also shows that the intrinsic error field may be one of the sources of the internal 3-D field perturbations. We need to further investigate higher n-modes to confirm if the characteristics of the triggered ELMs are really determined by the imposed 3-D fields, not by the possibility of most unstable modes at low-n numbers for the ELM occurrence in NSTX.

Acknowledgements

This work was funded by the US Department of Energy, contract numbers DE-AC05-000R22725, DE-AC52-07NA27344(LLNL), and DE-AC02-09CH11466. We thank A. Herrmann for use of the THEODOR heat conduction code.

References

[1] M. W. Jakubowski, T. E. Evans, M. E. Fenstermacher, *et al*, Nucl. Fusion **49** (2009) 095013

[2] J-W. Ahn, J. M. Canik, R. Maingi, *et al*, Nucl. Fusion **50** (2010), 045010

[3] T. E. Evans, R. K. W. Roeder, J. A. Carter, B. I. Rapoport, M. E. Fenstermacher and C. J. Lasnier, J. Phys : Conf. Ser. **7** (2005) 174-90

[4] T. E. Evans, R. A. Moyer, K. H. Burrell, *et al*, Nature Phys. 2 (2006) 419-23

[5] Y. Liang, H. R. Koslowski, P. R. Thomas, *et al*, Nucl. Fusion 50 (2010), 025013

[6] A. Kirk, E. Nardon, R. Akers, *et al*, Nucl. Fusion 50 (2010), 034008

[7] R. Maingi, T. H. Osborne, B. P. LeBlanc, *et al*, Phys. Rev. Lett. **103** (2009) 075001

[8] J. M. Canik, R. Maingi, T. E. Evnas, *et al*, Phys. Rev. Letts. **104** (2010) 045001

[9] J. M. Canik, R. Maingi, T. E. Evnas, *et al*, Nucl. Fusion **50** (2010) 034012

[10] J-W. Ahn, R. Maingi, D. Mastrovito, and A. L. Roquemore, Rev. Sci. Instrum. **81** (2010) 023501

[11] A. Herrmann, W. Junker, K. Gunther, *et al*, Plasma Phys. Control. Fusion **37** (1995) 17

[12] V. A. Soukhanovskii, A. L. Roquemore, C. H. Skinner, *et al*, Rev. Sci. Instrum. **74** (2003) 2094

[13] J.-K. Park, , A. H. Boozer, and A. H. Glasser, *et al*, Phys. Plasmas **14** (2007) 052110

[14] J. E. Menard, R. E. Bell, D. A. Gates, *et al*, Nucl. Fusion **50** (2010), 045008